Table I. Primer sequences for *PAX3*.

Exon 1	Forward	5'-TGTAAAACGACGGCCAGTAGAGCAGCGCGCTCCATTTG-3'
	Reverse	5'-CAGGAAACAGCTATGACCGCTCGCCGTGGCTCTCTGA-3'
Exon 2	Forward	5'-TGTAAAACGACGGCCAGTAAGAAGTGTCCAGGGCGCGT-3'
	Reverse	5'-CAGGAAACAGCTATGACCGGTCTGGGTCTGGGAGTCCG-3'
Exon 3	Forward	5'-TGTAAAACGACGGCCAGTTAAACGCTCTGCCTCCGCCT-3'
	Reverse	5'-CAGGAAACAGCTATGACCGGGATGTGTTCTGGTCTGCCC-3'
Exon 4	Forward	5'-TGTAAAACGACGGCCAGTAATGGCAACAGAGTGAGAGCTTCC-3'
	Reverse	5'-CAGGAAACAGCTATGACCAGGAGACACCCGCGAGCAGT-3'
Exon 5	Forward	5'-TGTAAAACGACGGCCAGTGGTGCCAGCACTCTAAGAACCCA-3'
	Reverse	5'-CAGGAAACAGCTATGACCGGTGATCTGACGGCAGCCAA-3'
Exon 6	Forward	5'-TGTAAAACGACGGCCAGTTGCATCCCTAGTAAAGGGCCA-3'
	Reverse	5'-CAGGAAACAGCTATGACCGGTGTCCATGGAAGACATTGGG-3'
Exon 7	Forward	5'-AACTATTATTTCATCAGTGAAATC-3'
	Reverse	5'-ATTCACTTGTATAAAATATCCACC-3'
Exon 8	Forward	5'-TGTAAAACGACGGCCAGTTGAAGCCAGTAGGAAGGGTGGA-3'
	Reverse	5'-CAGGAAACAGCTATGACCTGCAGGTTAAGAAACGCAGTTTGA-3'
Exon 9a	Forward	5'-TGTAAAACGACGGCCAGTTTGATACCGGCATGTGTGGC-3'
	Reverse	5'-CAGGAAACAGCTATGACCTGCAGTCAGATGTTATCGTCGGG-3'
Exon 9b	Forward	5'-TGTAAAACGACGGCCAGTCACAACTTTGTGTCCCTGGGATT-3'
	Reverse	5'-CAGGAAACAGCTATGACCGGGACTCCTGACCAACCACG-3'
Exon 10–11	Forward	5'-TGTAAAACGACGGCCAGTGCAAATGGAATGTTCTAGCTCCTCG-3'
	Reverse	5'-CAGGAAACAGCTATGACCGGTCAGCTCCAGGATCATATGGG-3'

sequences of the PAX3 and PAX5 paired domains were 79% homologous. The predicted PAX3 structure and the p.I59F mutation structure were superimposed on the backbone atoms of the PAX5 paired domain-DNA complex and displayed using the extensible visualization system, UCSF Chimera [12].

Results

In family 1, the proband, a 9-month-old male, was the first child of unrelated Japanese parents. Abnormal responses were found upon newborn hearing screening in the left ear, and left hearing loss was diagnosed by ABR. On physical examination, dystopia canthorum was noted, with a W-index of 2.77. The patient's mother also had dystopia canthorum, with a W-index of 2.68. She also had a history of early graying that started at age 16 years. She had not been diagnosed with WS1. According to the parents, 10 members of this family, including the proband and the mother, showed clinical features consistent with WS1 (Figure 1). ABR performed in the proband

a. heterochromia irides   b. congenital hearing loss
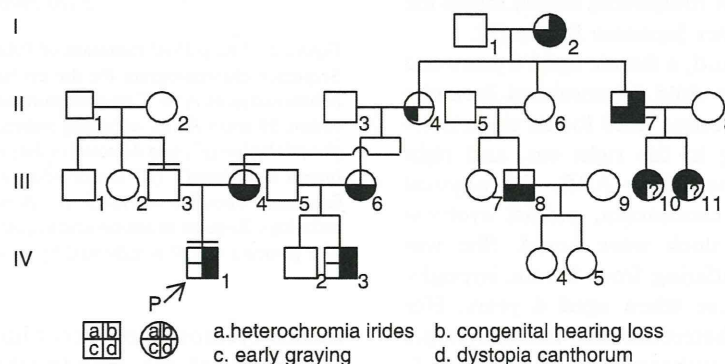c. early graying   d. dystopia canthorum

Figure 1. Pedigree of family 1. The proband is indicated by an arrow. The individuals we examined personally are indicated by a bar over the symbol. Phenotypes observed in this family are indicated symbolically as detailed below the pedigree.

revealed normal hearing in the right ear and no responses to 105 dB click stimuli in the left ear. Computed tomography (CT) of the temporal bone showed normal structures in the inner, middle, and outer ears.

Genetic analysis of *PAX3* was conducted in this family, and direct sequencing of *PAX3* revealed a heterozygous mutation, c.175A>T, in the proband and his mother. This mutation resulted in a missense mutation, p.I59F (Figure 2A). The proband's father did not harbor this mutation. p.I59F is located within exon 2 and is part of the paired domain of *PAX3*, which is a critical region for interaction between transcription factors and target DNA (Figure 2B). A multiple alignment of *PAX3* orthologs at this region demonstrated that I59 was evolutionarily conserved among various species (Figure 2C). The p.I59F mutation was not identified in any of the 184 alleles from the normal control subjects. This mutation was predicted to be 'probably damaging' according to PolyPhen-2 software.

The predicted 3D structures of the paired domain of the PAX3-DNA complex indicated that the PAX3 paired domain binds to the corresponding DNA (white double helixes) via hydrogen bonds (pink lines) at the N-terminal of α-helix1 (H1), α-helix2 (H2), and α-helix3 (H3) (indicated in blue; Figure 3A). I59 is located in the middle of H1, H2, and H3 and is surrounded by hydrophobic residues (green) protruding from H1, H2, and H3. Because the van der Waals radius of phenylalanine (Figure 3C; white arrows) is larger than that of iso-leucine (Figure 3B; white arrowheads), F59 repels the surrounding hydrophobic residues by van der Waals forces and increases the distance between F59 and the surrounding hydrophobic residues, resulting in struc-tural distortion of the DNA-binding site of PAX3. Since this site is precisely shaped for maximal binding to the corresponding DNA, this mutation is likely to reduce the binding ability of the paired domain of PAX3 and cause WSI. A mutational search found the same mutation in another Japanese family [8].

In family 2, the proband, a female aged 4 years and 4 months, was the first child of unrelated Japanese parents. Abnormal responses were found upon new-born hearing screening in the right ear, and right hearing loss was diagnosed by ABR. On physical examination, dystopia canthorum, medial eyebrow flare, and a white forelock were noted. She was admitted to hospital suffering from ketotic hypogly-cemia of unknown cause when aged 4 years. Her mother presented with heterochromia iridis, dystopia canthorum, and medial eyebrow flare, and her grand-mother presented with early graying that started at around 20 years of age, dystopia canthorum, and
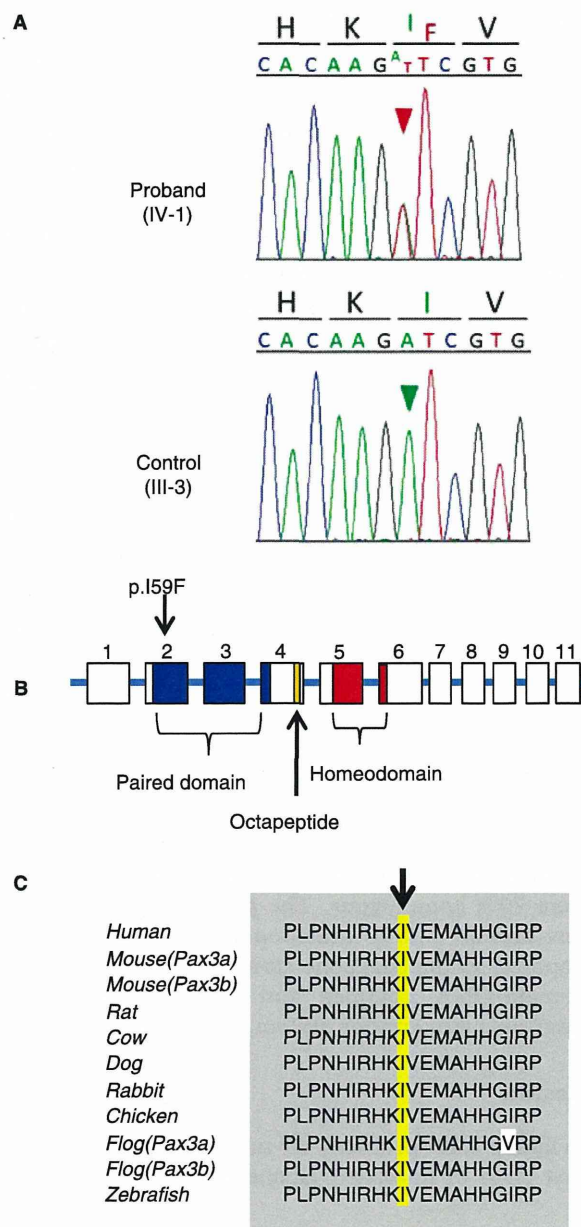

Figure 2. The p.I59F mutation of *PAX3* detected in family 1. (A) Sequence chromatogram for the proband and unaffected control. A heterozygous A to T transversion (red arrowhead) that changes codon 59 from ATC, encoding isoleucine (I), to TTC, encoding phenylalanine (F), was detected in the proband but not in the control (green arrowhead). (B) Localization of the p.I59F mutation and functional domains of PAX3. (C) A multiple alignment of PAX3 orthologs. Regions of amino acid sequence identity are shaded gray. The position of I59 is indicated by an arrow and shaded yellow.

medial eyebrow flare. According to the grandmother, the father of the grandmother also had dystopia canthorum and medial eyebrow flare. The pedigree of family 2 is shown in Figure 4. The grandmother
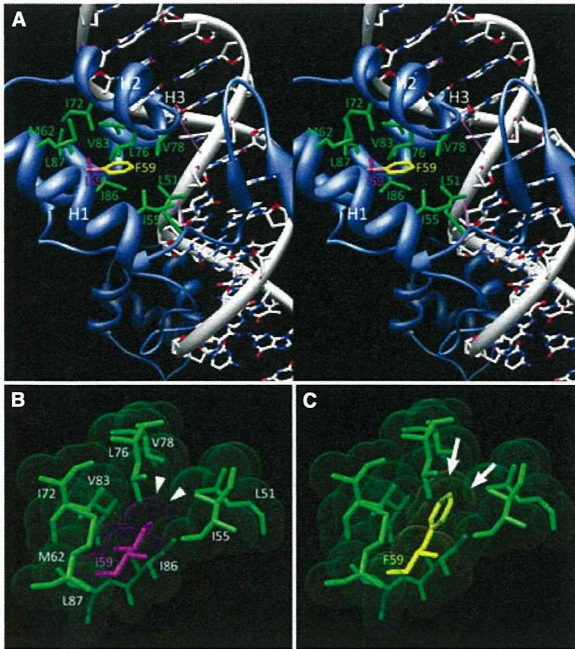
Figure 3. The predicted structure of the PAX3 paired domain-DNA complex. (A) The stereo view indicates that the mutated residue was surrounded by hydrophobic residues (green) protruding from H1, H2, and H3 of the paired domain (blue), which binds to DNA (white, sugar; blue, nitrogen; red, oxygen). The pink lines indicate hydrogen bonds. Magenta and yellow residues indicate I59 and F59, respectively. (B, C) The colored spheres indicate the van der Waals surface boundaries, the radius of the hydrophobic residues is shown in green, I59 is shown in magenta and is also indicated by arrowheads, and F59 is shown in yellow and is also indicated by arrows.

and her father had never been diagnosed with WS1. Pure tone audiometry of the proband showed severe hearing loss in the right ear and normal hearing in the left ear. The results of ABR and distortion product

otoacoustic emissions in the proband were compatible with those obtained for pure tone audiometry.

Because direct sequencing of *PAX3* in the proband and her grandmother revealed no mutations, we conducted MLPA analysis to search for a large deletion of *PAX3*, and found that the copy number of all tested exons (exons 1–9) of *PAX3* was half that of the number of other chromosomal regions in both subjects (Figure 5A). In control subjects, all tested exons of *PAX3* showed the same copy number as the other chromosomal regions (Figure 5B). To determine the size of the deleted region, quantitative PCR was performed at 12 sequence-tagged sites on chromosome 2q36, which includes *PAX3*. In the proband, copy numbers at nine sites in the middle of the tested region (white arrows) were half that of those examined in normal controls, but the copy numbers at three of the sites near the 5' and 3' ends of the tested region (black arrows) were identical to those examined in normal controls (Figure 6). This result demonstrated that the chromosomal region spanning 1759–2554 kb at 2q36, which includes the whole *PAX3* gene, was deleted in one of the alleles of the proband. The same results were detected in the grandmother. A search for the deleted region revealed that this region contained between 12 and 18 genes, including *PAX3*.

Discussion

The heterozygous missense mutation, p.I59F, was identified in family 1. The pathogenicity of a novel or rare missense mutation in the causative gene is not necessarily verified even when the mutation is absent from a large number of normal controls, when the residue is evolutionary conserved among different species, or if the mutation is associated with the phenotype within a family, because an identified
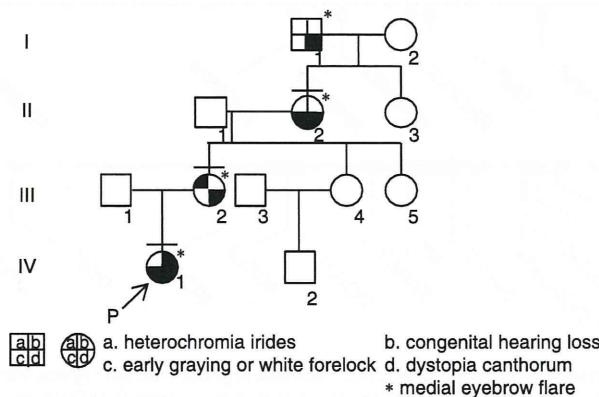

Figure 4. Pedigree of family 2. The proband is indicated by an arrow. The individuals we examined personally are indicated by a bar over the symbol. Phenotypes observed in this family are indicated symbolically, as detailed below the pedigree.

a. heterochromia irides
b. congenital hearing loss
c. early graying or white forelock
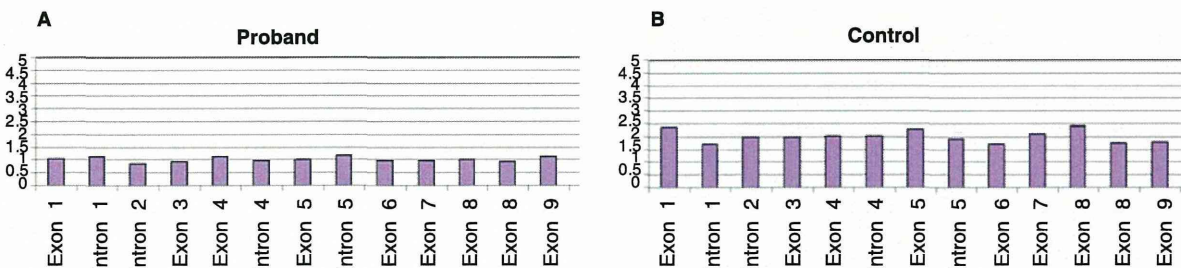d. dystopia canthorum
* medial eyebrow flare

Figure 5. Results of MLPA analysis of *PAX3* in family 2. (A, B) Relative ratios of DNA quantity in each exon compared with that in the control region are shown for the proband (A) and control (B).

missense mutation may be a rare normal variant. Thus, the pathogenicity of such mutations needs to be verified by detection of the same mutation in multiple families with the same phenotype or by functional analysis. The functional consequences of a few *PAX3* mutations have been tested and reduced DNA-binding properties have been reported [13–15]. The p.I59F mutation was reported in a Japanese family [8], but functional analysis has not been conducted. We analyzed the predicted 3D structures of the paired domain of the PAX3-DNA complex and showed that this mutation was likely to distort the structure of the DNA-binding site of PAX3 and lead to functional impairment. This result substantially supports the hypothesis that the p.I59F mutation is pathogenic, although it is based on a theoretical prediction rather than functional experiments.

In family 2, the distinct phenotypes of the proband, the proband's mother, and the proband's grandmother were congenital unilateral hearing loss, heterochromia iridis, and early graying, respectively. Because of these differences, they were not aware of the hereditary nature of the symptoms. Identification of the *PAX3* mutation in the proband and the proband's grandmother led to an accurate diagnosis of WS1 and facilitated understanding of the symptoms. In this family, direct sequencing of *PAX3* did not detect any mutations, but MLPA analysis detected a large heterozygous deletion. Furthermore, quantitative PCR analysis revealed that the deleted region spanned 1759–2554 kb and included 12–18 genes. Large deletions of *PAX3* in patients with WS1 have been reported in several families [6,16–18]. To our knowledge, however, this is the largest deletion identified in patients with WS1 and has, therefore, expanded the spectrum of *PAX3* mutations. There is no reported correlation between the nature of the mutation (deleted vs truncated or missense) or
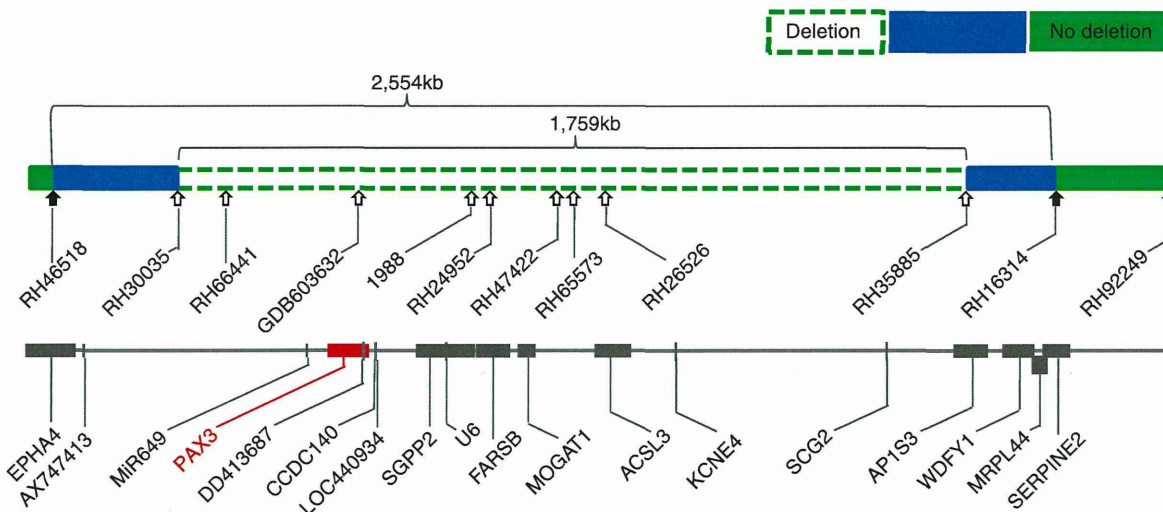

Figure 6. Genetic map showing the estimated location of the *PAX3* deletion together with the regions surrounding *PAX3*. Sites examined by quantitative PCR are indicated by arrows. Blank and white arrows indicate that the quantities of DNA at these sites are half or identical to the quantities of DNA at the corresponding sites in the control, respectively. The 5′ and 3′ ends of the deletion are located within the blue regions flanking the white region, designated as 'deletion,' and flanked by the green regions, designated as 'no deletion.' All genes mapped within this region, including *PAX3*, are shown in the lower map.

its location in *PAX3*, and the severity of the WS1 phenotype [19,20]. Similarly, no evidence of such a correlation was found in the data presented in this study.

In the present study, *PAX3* genetic diagnosis contributed to the accurate diagnosis of WS1. Such diagnosis could help provide genetic counseling to patients with isolated or few phenotypic symptoms, those with mild phenotypes or few first-degree relatives, or those who have yet to develop any symptoms. In addition, analysis of the predicted 3D structure of PAX3 facilitated the verification of pathogenicity of a missense mutation, and MLPA analysis increased the sensitivity of genetic diagnosis of WS1.

Acknowledgments

Declaration of interest: The authors report no conflicts of interest. The authors alone are responsible for the content and writing of the paper.

References

[1] Read AP, Newton VE. Waardenburg syndrome. J Med Genet 1997;34:656–65.

[2] Farrer LA, Grundfast KM, Amos J, Arnos KS, Asher JH Jr, Beighton P, et al. Waardenburg syndrome (WS) type I is caused by defects at multiple loci, one of which is near ALPP on chromosome 2: first report of the WS consortium. Am J Hum Genet 1992;50:902–13.

[3] Liu XZ, Newton VE, Read AP. Waardenburg syndrome type II: phenotypic findings and diagnostic criteria. Am J Med Genet 1995;55:95–100.

[4] Pardono E, van Bever Y, van den Ende J, Havrenne PC, Iughetti P, Maestrelli SR, et al. Waardenburg syndrome: clinical differentiation between types I and II. Am J Med Genet A 2003;117A:223–35.

[5] Pingault V, Ente D, Dastot-Le Moal F, Goossens M, Marlin S, Bondurand N. Review and update of mutations causing Waardenburg syndrome. Hum Mutat 2010;31: 391–406.

[6] Milunsky JM, Maher TA, Ito M, Milunsky A. The value of MLPA in Waardenburg syndrome. Genet Test 2007;11:179–82.

[7] Ishikiriyama S, Tonoki H, Shibuya Y, Chin S, Harada N, Abe K, et al. Waardenburg syndrome type I in a child with de novo inversion (2)(q35q37.3). Am J Med Genet 1989;33: 505–7.

[8] Soejima H, Fujimoto M, Tsukamoto K, Matsumoto N, Yoshiura KI, Fukushima Y, et al. Three novel PAX3 mutations observed in patients with Waardenburg syndrome type 1. Hum Mutat 1997;9:177–80.

[9] Kashima T, Akiyama H, Kishi S. Asymmetric severity of diabetic retinopathy in Waardenburg syndrome. Clin Ophthalmol 2011;5:1717–20.

[10] Kiefer F, Arnold K, Kunzli M, Bordoli L, Schwede T. The SWISS-MODEL Repository and associated resources. Nucleic Acids Res 2009;37:D387–92.

[11] Xu W, Rould MA, Jun S, Desplan C, Pabo CO. Crystal structure of a paired domain-DNA complex at 2.5 A resolution reveals structural basis for Pax developmental mutations. Cell 1995;80:639–50.

[12] Pettersen EF, Goddard TD, Huang CC, Couch GS, Greenblatt DM, Meng EC, et al. UCSF Chimera – a visualization system for exploratory research and analysis. J Comput Chem 2004;25:1605–12.

[13] Chalepakis G, Goulding M, Read A, Strachan T, Gruss P. Molecular basis of splotch and Waardenburg Pax-3-mutations. Proc Natl Acad Sci USA 1994;91:3685–9.

[14] Corry GN, Underhill DA. Pax3 target gene recognition occurs through distinct modes that are differentially affected by disease-associated mutations. Pigment Cell Res 2005;18: 427–38.

[15] Fortin AS, Underhill DA, Gros P. Reciprocal effect of Waardenburg syndrome mutations on DNA binding by the Pax-3 paired domain and homeodomain. Hum Mol Genet 1997;6:1781–90.

[16] Baldwin CT, Lipsky NR, Hoth CF, Cohen T, Mamuya W, Milunsky A. Mutations in PAX3 associated with Waardenburg syndrome type I. Hum Mutat 1994;3:205–11.

[17] Tassabehji M, Newton VE, Leverton K, Turnbull K, Seemanova E, Kunze J, et al. PAX3 gene structure and mutations: close analogies between Waardenburg syndrome and the Splotch mouse. Hum Mol Genet 1994;3: 1069–74.

[18] Wang J, Li S, Xiao X, Wang P, Guo X, Zhang Q. PAX3 mutations and clinical characteristics in Chinese patients with Waardenburg syndrome type 1. Mol Vis 2010;16:1146–53.

[19] Baldwin CT, Hoth CF, Macina RA, Milunsky A. Mutations in PAX3 that cause Waardenburg syndrome type I: ten new mutations and review of the literature. Am J Med Genet 1995;58:115–22.

[20] Tassabehji M, Newton VE, Liu XZ, Brady A, Donnai D, Krajewska-Walasek M, et al. The mutational spectrum in Waardenburg syndrome. Hum Mol Genet 1995;4: 2131–7.

Moderate hearing loss associated with a novel KCNQ4 non-truncating mutation located near the N-terminus of the pore helix

Takahisa Watabe [a], Tatsuo Matsunaga [b,*], Kazunori Namba [b], Hideki Mutai [b], Yasuhiro Inoue [a], Kaoru Ogawa [a]

[a] Department of Otolaryngology, Head and Neck Surgery, Keio University, School of Medicine, 35 Shinanomachi, Shinjuku, Tokyo 160-8582, Japan
[b] The Laboratory of Auditory Disorders, National Institute of Sensory Organs, National Tokyo Medical Center, 2-5-1 Higashigaoka, Meguro, Tokyo 152-8902, Japan

ABSTRACT

Genetic mutation is one of the causative factors for idiopathic progressive hearing loss. A patient with late-onset, moderate, and high-frequency hearing loss was found to have a novel, heterozygous KCNQ4 mutation, c.806_808delCCT, which led to a p.Ser260del located between S5 and the pore helix (PH). Molecular modeling analysis suggested that the p.Ser269del mutation could cause structural distortion and change in the electrostatic surface potential of the KCNQ4 channel protein, which may impede K+ transport. The present study supports the idea that a non-truncating mutation around the N-terminus of PH may be related to moderate hearing loss.

© 2013 Elsevier Inc. All rights reserved.

1. Introduction

Currently, 50 loci and 27 responsible genes for autosomal dominant non-syndromic hearing loss (DFNA) have been identified [1]. KCNQ4 is one gene that can cause DFNA, type 2 (DFNA2, OMIM: 600101) [2,3]. Patients with mutations in this gene present progressive sensorineural hearing loss starting in the high frequency range. KCNQ4 (OMIM: 603537) is a voltage-gated KQT-like potassium channel. It modulates the resting membrane potential of the outer hair cells, a type of auditory sensory cell. A functional KCNQ4 channel consists of four subunits. Each subunit contains six putative domains that span the cellular membrane (S1–S6), a K+-selective pore region consisting of S5, S6, a pore helix (PH), and a pore-loop (P-loop) domain, and N- and C-terminal regions [3].

So far, 11 missense mutations, one nonsense mutation, and three small deletion mutations in KCNQ4 have been reported to be associated with hearing loss. Understanding the molecular pathology resulting from each KCNQ4 mutation would be beneficial in predicting the clinical course of KCNQ-related hearing loss. KCNQ4 mutations can be divided into non-truncating and

truncating mutations (Table 1). Most of the KCNQ4 non-truncating mutations in the pore region are associated with severe hearing loss, except for a non-truncating mutation at the N-terminus of PH, p.Tyr270His, which has been associated with moderate hearing loss [13]. In an electrophysiological study, co-expression of wild-type KCNQ4 with each non-truncating mutation associated with severe hearing loss, including p.Leu274His, p.Trp276Ser, p.Leu281-Ser, p.Gly285Cys, p.Gly285Ser, p.Gly296Ser, p.Gly321Ser, and p.Gly322_Leu327del, has been shown to result in significantly reduced or non-detectable current [14]. These results indicate that the severe hearing loss in patients carrying these heterozygous mutations is due to a dominant negative effect. On the other hand, the protein products of two KCNQ4-truncating mutations, p.Gln71SerfsX138 and p.Gln71fs, lack structural motifs, such as transmembrane domains, and are probably not synthesized from these alleles. Moderate hearing loss in patients carrying these mutations in the heterozygous allele has been considered to be due to haploinsufficiency [3,11].

We identified a novel heterozygous KCNQ4 non-truncating mutation, c.806_808delCCT, that leads to deletion of a serine residue at position 269 (p.Ser269del), located in the region between S5 and the PH of the protein. Unlike other patients with KCNQ4 non-truncating mutations, the patient who carried this mutation presented moderate hearing loss. Previously, we reported that a patient having KCNQ4 with p.Try270His, which is located next to Ser269, showed moderate hearing loss [13], raising the possibility that mutation at or proximal to the N-terminus of PH is associated

Table 1
KCNQ4 mutations affecting the pore region of the channel protein in DFNA2 families.

	Exon		Nucleotide	Amino acid	Protein domain	Onset (y)	Progression	Severity	Mechanism	Refs.
Non-truncating mutation	5	Missense	c.778G>A	p.Glu260Lys	S5	1–20	Yes	SV	Unknown	[9]
	5		c.785A>T	p.Asp262Val	S5-PH	1–20	Yes	SV	Unknown	[9]
	5		c.808T>C	p.Tyr270His	N-terminus of PH	0	Yes	MD	Unknown	[13]
	5		c.821T>A	p.Leu274His	PH	1–20	Yes	SV	D.N.E.	[12]
	5		c.827G>C	p.Trp276Ser	PH	1–20	Yes	SV	D.N.E.	[3–5]
	6		c.842T>C	p.Leu281Ser	PH	1–20	Yes	SV	D.N.E.	[6]
	6		c.853G>T	p.Gly285Cys	P-loop	1–20	Yes	SV	D.N.E.	[3]
	6		c.853G>A	p.Gly285Ser	P-loop	1–20	Yes	SV	D.N.E.	[2]
	6		c.859G>C	p.Gly287Arg	P-loop	1–20	Yes	SV	D.N.E.	[7]
	6		c.886G>A	p.Gly296Ser	S6	1–20	Yes	SV	D.N.E.	[8]
	7		c.961G>A	p.Gly321Ser	S6	1–20	Yes	SV	D.N.E.	[3]
	4	Deletion	c.664_681del18	p.Gly322_Leu327del	S5	1–20	Yes	SV	D.N.E.	[10]
	5		c.806_808del3	p.Ser269del	S5-PH	1–20	Yes	MD	See discussion	This study
Truncating mutation	1	Deletion	c.211del1	p.Gln71SerfsX138	N-terminal cytoplasmic	Unknown	Yes	MD	H.I.?	[11]
	1		c.212_224del13	p.Gln71fs	N-terminal cytoplasmic	1–20	Yes	MD	H.I.?	[3]
	5	Nonsense	c.725G>A	p.Trp242X	S5	1–20	Unknown	SV	Unknown	[9]

SV: severe, MD: moderate D.N.E.: dominant negative effect, H.I.: haploinsufficiency, PH: pore helix.

with moderate hearing loss. In this study, we used molecular modeling to elucidate the molecular mechanism underlying moderate hearing loss associated with KCNQ4 harboring the p.Ser269del mutation.

2. Materials and methods

2.1. Subjects

All procedures were approved by the Ethics Review Committee of National Mie Hospital and National Tokyo Medical Center, and were conducted after written informed consent had been obtained from each individual.

2.2. Clinical analysis

Hearing level was measured by pure tone audiometry and evaluated by averaging four frequencies, 500, 1000, 2000, and 4000 Hz in the better hearing ear and was classified according to the criteria of GENDEAF (moderate, 41–70 dB; severe, 71–95 dB) [1]. Clinical information, such as age of onset and presence of progression, was gathered from the medical records. Computed tomography (CT) and magnetic resonance imaging (MRI) were done to check whether the patient had an inner ear anomaly and/or retrocochlear disease. Auditory brainstem response (ABR) and distortion product otoacoustic emission (DPOAE) were also examined to evaluate inner ear function.

2.3. Genetic analysis

KCNQ4 was selected as the candidate gene on the basis of clinical features, including onset of hearing loss, audiogram patterns, imaging studies, and hereditary pattern [15]. Prior to this study, the patient was confirmed to have neither GJB2 mutations, the most common causative gene of hereditary hearing loss, nor mitochondrial m.1555A>G and m.3243A>G mutations. Genomic DNA was extracted from blood samples using the Gentra Puregene Blood kit (QIAGEN, Hamburg, Germany). PCR primers specific for KCNQ4 (GenBank NG_008139, NCBI Build37.1) were selected from the resequencing amplicon probe sets (NCBI). All of the exons, together with the flanking intronic regions, of KCNQ4 were analyzed by bidirectional sequencing using an ABI 3730 Genetic Analyzer (Applied Biosystems, CA, USA) and the ABI Prism Big Dye Terminator Cycle Sequencing kit (Applied Biosystems). The sequences were characterized using SeqScape software v.2.6 (Applied Biosystems)

and DNASIS Pro (Hitachisoft, Tokyo, Japan). Control DNA was obtained from 96 Japanese subjects with normal hearing.

2.4. Molecular model analysis

To predict the effects of the mutation on the KCNQ4 channel, molecular modeling of KCNQ4 was performed as previously described [13]. The crystal structure of Kv1.2 (PDB ID: 3LUT, chain B) [16] was used as the structural template for modeling of the KCNQ4 sequence based on sequence homology as determined through Gapped BLAST [17] and PDBsum [18]. The pore regions of wild-type KCNQ4 and the p.Ser269del mutation were modeled using SWISS-MODEL Workspace [19] and validated using the Verify 3D Structure Evaluation server [20,21]. The models were each superimposed onto Kv1.2 using Chimera [22] to visualize ribbon models with electrostatic surface potentials and the hydrogen bonds of either wild-type KCNQ4 or KCNQ4 with the p.Ser269del mutation.

3. Results

3.1. Clinical features

The proband was a 25-years-old female in a pedigree of autosomal dominant progressive hearing loss (Fig. 1A). She has become conscious of progressive bilateral hearing loss, since she has become 20 years-old. At 24 years-old, severe mixed hearing loss with high frequency dominance was found in the right ear by pure tone audiometry. An air-bone gap was considered to have resulted from an operation for a right cholesteatoma at 8 years of age. Moderate sensorineural hearing loss with high frequency dominance was found in the left ear (Fig. 1B). No other symptoms accompanying the hearing loss were identified. ABR showed a threshold of 90 dB in the left ear, and no response at 90 dB in the right ear. DPOAE showed a response only at 1000 Hz in the left ear and no response in the right ear. CT and MRI failed to reveal deformity of the inner ear or structural abnormality in the central auditory pathway.

3.2. Novel mutation of KCNQ4

Sequencing analysis of KCNQ4 from the patient identified a heterozygous deletion of three nucleotides, CCT, at position 806–808 (c.806_808delCCT). The deletion mutation causes a change of amino acid residues from Ser268-Ser269-Tyr270 to Ser268-Tyr269 (p.Ser269del) without a frameshift (Fig. 2A). Ser269 was located
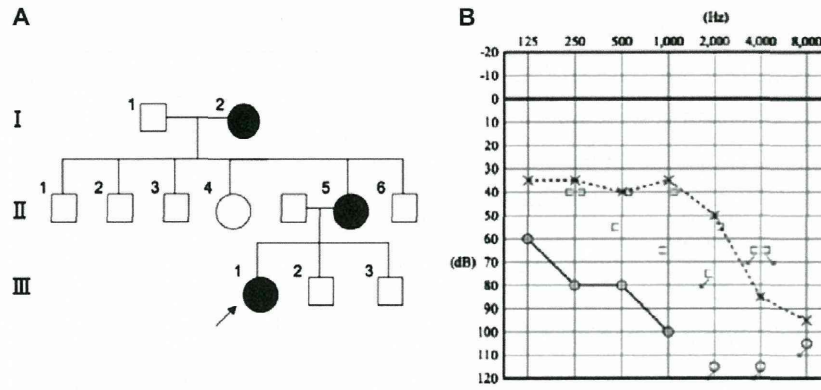
Fig. 1. Clinical information. (A) Pedigree of a family carrying heterozygous *KCNQ4* with the c.806_808delCCT (p.Ser269del) mutation. Individuals with hearing loss are indicated by filled symbols. The arrow indicates the proband. (B) Pure tone audiogram from the proband at 25 years old. Open circles with line: air conduction thresholds of the right ear; x with dotted line: air conduction thresholds of the left ear; left bracket: bone conduction thresholds of the right ear; right bracket: bone conduction thresholds of the left ear. Arrows indicate the non-detectable hearing level by profound hearing loss.
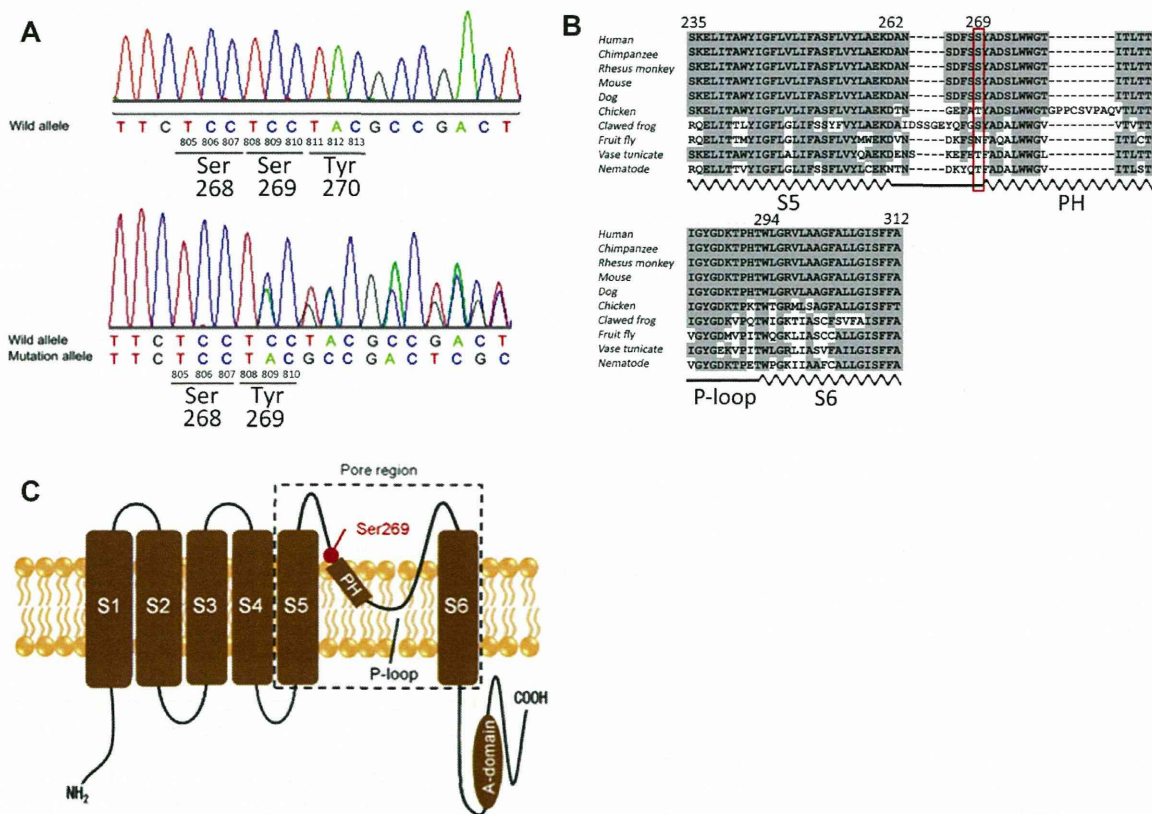

Fig. 2. Partial electrophoretogram of exon 5 of *KCNQ4* with the partial protein sequence for *KCNQ4*. (A) A partial electrophoretogram of exon 5 of *KCNQ4* from an individual with normal hearing (above) and the proband with the heterozygous c.806–808delCCT mutation (below). The positions of the heterozygotic deletion of CCT at 806–808 and the resulting amino acid deletion (p.Ser269del) are indicated. (B) Sequences of the orthologous *KCNQ4* pore region are aligned. Positions highlighted in gray indicate the residues identical to human *KCNQ4*. The position of Ser269 is enclosed by a red square. The positions of S5, pore helix (PH), S6 (wavy lines) and the P-loop (straight line) are shown below the sequences. (C) Schematic topology of *KCNQ4*. Putative domains, including transmembrane regions (S1-S6), channel pore region, PH, P-loop, and A-domain are indicated. Position of Ser269 is indicated by a red circle. (For interpretation of the references to color in this figure legend, the reader is referred to the web version of this article.)

in the region between the putative S5 and PH, a highly conserved region among animal species (Fig. 2B and C). This mutation was found neither on the Exome Variant Server [23] nor in the control group of 96 unrelated Japanese individuals with normal hearing.
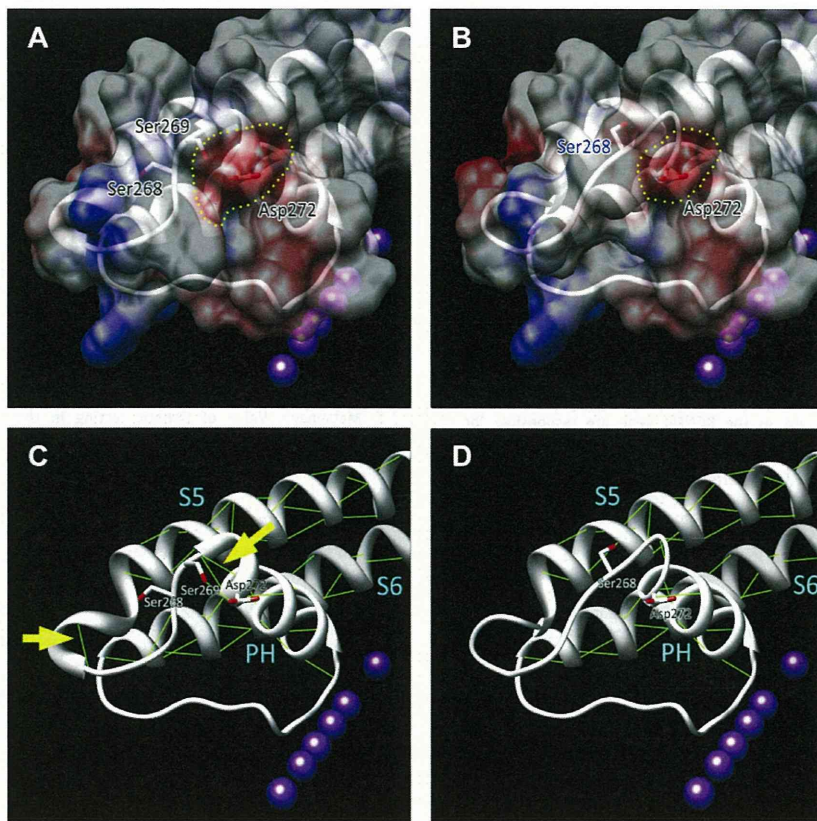
Fig. 3. Partial structural model of KCNQ4 and the p.Ser269del mutation. (A and B) The ribbon models of (A) wild-type KCNQ4 subunit and (B) KCNQ4 subunit with the p.Ser269del mutation overlaid with their corresponding electrostatic surface potential. Red or blue area: negatively or positively charged residues, yellow dot circle: negatively charged surface potential on the N-terminal region of the pore helix (PH). (C and D) Ribbon models of (C) wild-type KCNQ4 and (D) KCNQ4 with the p.Ser269del mutation. Green lines: putative hydrogen bonds; yellow arrows: hydrogen bonds within S5 and PH; purple spheres: potassium ions. (For interpretation of the references to color in this figure legend, the reader is referred to the web version of this article.)

3.3. Predicted structural change in KCNQ4 caused by the p.Ser269del mutation

The ribbon model of the wild-type KCNQ4 subunit overlaid with the corresponding electrostatic surface potential demonstrated that the surface of the N-terminal region of PH is negatively charged because of the negatively charged side chains of Ser269 and Asp272 (Fig. 3A). The model of KCNQ4 with the p.Ser269del mutation demonstrated reduction of the negatively charged surface area in this region (Fig. 3B). Reduction of the electrostatic surface potential in this area has been predicted to impede K+ transport because of the long range electrostatic attractive force between PH and K+ [13]. In addition, hydrogen bonds on the C-terminus of S5 and the N-terminus of PH of wild-type KCNQ4 (Fig. 3C, yellow arrows) were absent in KCNQ4 with the Ser269del mutation (Fig. 3D). Loss of the hydrogen bonds around the N-terminus of PH resulted in shortening of the PH and was attributed to destabilization of α-helix formation [24]. The disrupted helices would affect the structural stability of the pore region and lead to abnormal channel function.

4. Discussion

Most of the KCNQ4 non-truncating mutations affecting the pore region are associated with severe hearing loss. However, we found that the non-truncating p.Tyr270His [14] and p.Ser269del muta-

tions were associated with moderate hearing loss. KCNQ4 mutations at or proximal to the N-terminus of PH are suggested to be associated with moderate hearing loss, because this site is predicted to have relatively smaller influence than other pore regions, such as S5, S6, the central region of PH, and the P-loop, on KCNQ4 channel function.

The molecular pathology associated with the p.Ser269del mutation, demonstrated in silico, indicates a reduction in the negatively charged electrostatic surface potential and structural distortion of the pore region by the mutated KCNQ4, which may explain the associated moderate hearing loss. The molecular mechanism in this case is likely to be a mild dominant negative effect resulting from the relatively small influence of KCNQ4 with the p.Ser269del mutation on the normal channel subunit. However, another possibility is haploinsufficiency resulting from the loss of function of KCNQ4 with the p.Ser269del mutation. This scenario, which would not affect the functioning of the other channel subunits, cannot be excluded.

5. Conclusion

We found a novel heterozygous KCNQ4 mutation, c.806_808del-CCT (p.Ser269del), in a pedigree with progressive and moderate hearing loss. Molecular modeling analysis of this mutation demonstrated that changes in electrostatic surface potential and structural distortion could be relevant to the pathology underlying

auditory dysfunction. Mutations at or proximal to the N-terminus of the PH of the KCNQ4 channel might cause mild molecular dysfunction and be associated with moderate hearing loss.

Acknowledgment

References

[1] <http://hereditaryhearingloss.org/> (accessed September 2012).
[2] C. Kubisch, B.C. Schroeder, T. Friedrich, B. Lütjohann, A. El Amraoui, S. Marlin, C. Petit, T.J. Jentsch, KCNQ4, a novel potassium channel expressed in sensory outer hair cells, is mutated in dominant deafness, Cell 96 (1999) 437–446.
[3] P.J. Coucke, P. Van Hauwe, P.M. Kelley, H. Kunst, I. Schatteman, D. Van Velzen, J. Meyers, R.J. Ensink, M. Verstreken, F. Declau, H. Marres, K. Kastury, S. Bhasin, W.T. McGuirt, R.J. Smith, C.W. Cremers, P. Van de Heyning, P.J. Willems, S.D. Smith, G. Van Camp, Mutations in the KCNQ4 gene are responsible for autosomal dominant deafness in four DFNA2 families, Hum. Mol. Genet. 8 (1999) 1321–1328.
[4] J. Akita, S. Abe, H. Shinkawa, W.J. Kimberling, S. Usami, Clinical and genetic features of nonsyndromic autosomal dominant sensorineural hearing loss: KCNQ4 is a gene responsible in japanese, J. Hum. Genet. 46 (2001) 355–361.
[5] G. Van Camp, P.J. Coucke, J. Akita, E. Fransen, S. Abe, E.M. De Leenheer, P.L. Huygen, C.W. Cremers, S. Usami, A mutational hot spot in the KCNQ4 gene responsible for autosomal dominant hearing impairment, Hum. Mutat. 20 (2002) 15–19.
[6] Z. Talebizadeh, P.M. Kelley, J.W. Askew, K.W. Beisel, S.D. Smith, Novel Mutation in the KCNQ4 Gene in a large kindred with dominant progressive hearing loss, Hum. Mutat. 14 (1999) 493–501.
[7] J. Arnett, S.B. Emery, T.B. Kim, A.K. Boerst, K. Lee, S.M. Leal, M.M. Lesperance, Autosomal dominant progressive sensorineural hearing loss due to a novel mutation in the KCNQ4 gene, Arch. Otolaryngol. Head Neck Surg. 137 (2011) 54–59.
[8] A. Mencía, D. González-Nieto, S. Modamio-Høybjør, A. Etxeberría, G. Aránguez, N. Salvador, I. Del Castillo, A. Villarroel, F. Moreno, L. Barrio, M.A. Moreno-Pelayo, A novel KCNQ4 pore-region mutation (p.G296S) causes deafness by impairing cell-surface channel expression, Hum. Genet. 123 (2008) 41–53.
[9] M.S. Hildebrand, D. Tack, S.J. McMordie, A. DeLuca, I.A. Hur, C. Nishimura, P. Huygen, T.L. Casavant, R.J. Smith, Audioprofile-directed screening identifies novel mutations in KCNQ4 causing hearing loss at the DFNA2 locus, Genet. Med. 10 (2008) 797–804.
[10] J.I. Baek, H.J. Park, K. Park, S.J. Choi, K.Y. Lee, J.H. Yi, T.B. Friedman, D. Drayna, K.S. Shin, U.K. Kim, Pathogenic effects of a novel mutation (c.664_681del) in KCNQ4 channels associated with auditory pathology, Biochim. Biophys. Acta 2011 (1812) 536–543.
[11] F. Kamada, S. Kure, T. Kudo, Y. Suzuki, T. Oshima, A. Ichinohe, K. Kojima, T. Niihori, J. Kanno, Y. Narumi, A. Narisawa, K. Kato, Y. Aoki, K. Ikeda, T. Kobayashi, Y. Matsubara, A novel KCNQ4 one-base deletion in a large pedigree with hearing loss: implication for the genotype-phenotype correlation, J. Hum. Genet. 51 (2006) 455–460.
[12] P. Van Hauwe, P.J. Coucke, R.J. Ensink, P. Huygen, C.W. Cremers, G. Van Camp, Mutations in the KCNQ4 K+ channel gene, responsible for autosomal dominant hearing loss, cluster in the channel pore region, Am. J. Med. Genet. 93 (2000) 184–187.
[13] K. Namba, H. Mutai, H. Kaneko, S. Hashimoto, T. Matsunaga, In silico modeling of the pore region of a KCNQ4 missense mutant from a patient with hearing loss, BMC Res. Notes 5 (2012) 145.
[14] H.J. Kim, P. Lv, C.R. Sihn, E.N. Yamoah, Cellular and molecular mechanisms of autosomal dominant form of progressive hearing loss, DFNA2, J. Biol. Chem. 286 (2011) 1517–1527.
[15] T. Matsunaga, Value of Genetic testing in the ontological approach for sensorineural hearing loss, Keio J. Med. 58 (2009) 216–222.
[16] X. Chen, Q. Wang, F. Ni, J. Ma, Structure of the full-length shaker potassium channel Kv1.2 by normal-mode-based X-ray crystallographic refinement, Proc. Natl. Acad. Sci. USA 107 (2010) 11352–11357.
[17] S.F. Altschul, T.L. Madden, A.A. Schäffer, J. Zhang, Z. Zhang, W. Miller, D.J. Lipman, Gapped BLAST and PSI-BLAST: a new generation of protein database search programs, Nucleic Acids Res. 25 (1997) 3389–3402.
[18] R.A. Laskowski, Enhancing the functional annotation of PDB structures in PDBsum using key figures extracted from the literature, Bioinformatics 23 (2007) 1824–1827.
[19] <http://swissmodel.expasy.org/> (accessed November 2012).
[20] <http://nihserver.mbi.ucla.edu/Verify_3D> (accessed November 2012).
[21] K. Arnold, L. Bordoli, J. Kopp, T. Schwede, The SWISS-MODEL workspace: a web-based environment for protein structure homology modeling, Bioinformatics 22 (2006) 195–201.
[22] E.F. Pettersen, T.D. Goddard, C.C. Huang, G.S. Couch, D.M. Greenblatt, E.C. Meng, T.E. Ferrin, UCSF Chimera – a visualization system for exploratory research and analysis, J. Comput. Chem. 25 (2004) 1605–1612.
[23] <http://evs.gs.washington.edu/EVS/> (accessed August 2012).
[24] W.G. Hol, Effects of the alpha-helix dipole upon the functioning and structure of proteins and peptides, Adv. Biophys. 19 (1985) 133–165.